Karlsruhe Institute of Technology

Overview of the Micro-bunching Instability in Electron Storage Rings and Evolving Diagnostics

12th International Particle Accelerator Conference - IPAC'21

Miriam Brosi | 27 May 2021

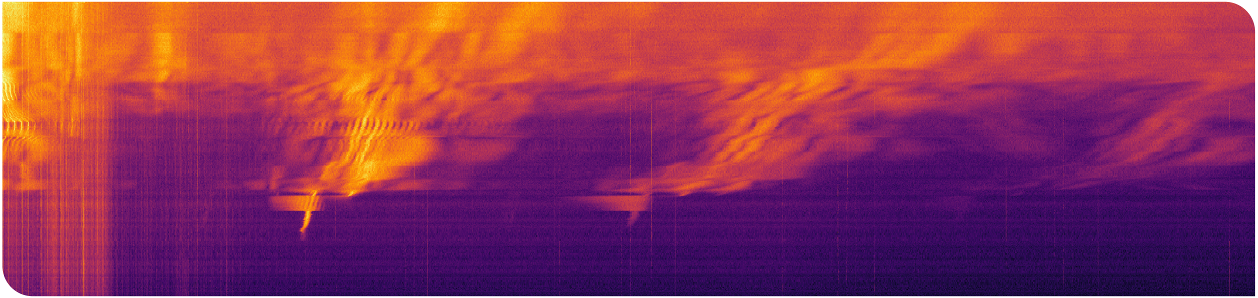

Micro-bunching Instability

- Longitudinal coherent instability
- Self-interaction between bunch and emitted coherent synchrotron radiation (CSR)
- Occuring for short bunch length
- Substructures in the longitudinal phase space
  → Deformation of bunch profile and energy distribution
  → Change in emitted CSR spectrum
- Dynamic bursts due to rising and damping of substructures
- Observed amongst others at ALS [1], ANKA [2], BESSY II [3], CLS [4], DIAMOND [5], Elettra [6], MAX-I [7], MLS [8], NewSUBARU [9], NSLS VUV Ring [10], UVSOR-II [11], SLC damping ring [12], SOLEIL [13], SURF III [14]

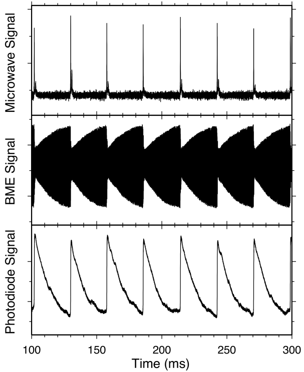

Observed bursts on microwave signal (CSR), beam monitor electrode signal (inversely proportional to bunch length) and photodiode signal (proportional to energy spread)
U. Arp, doi:10.1103/PhysRevSTAB.4.054401 [14]

Examples at different facilities

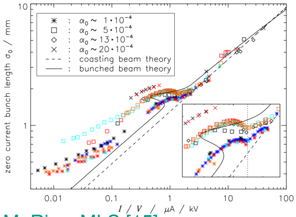

M. Ries, MLS [15]

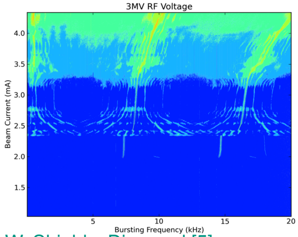

W. Shields, Diamond [5]

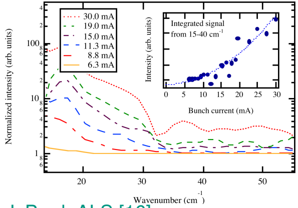

J. Byrd, ALS [16]

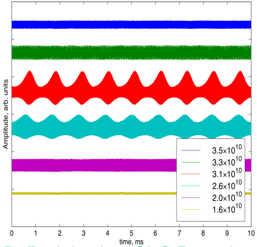

B. Podobedov, SLC Damping rings [17]

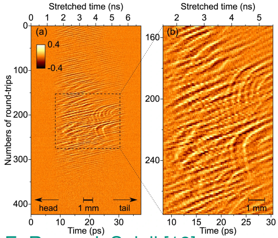

E. Roussel, Soleil [18]

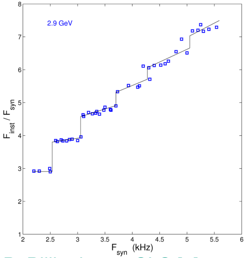

B. Billinghurst, CLS [4]

Content

- Theory
- Simulation
- Diagnostics
- Measurements
  - Synchronous measurements
  - Current dependence
  - Dependence on operational parameters
  - Multi-bunch operation
- Snapshot measurement method
- Ongoing work
- Summary

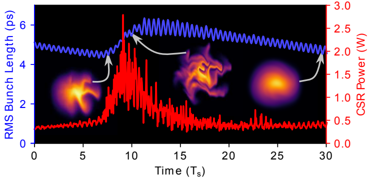

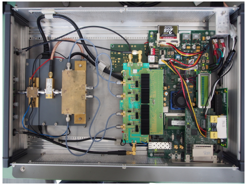

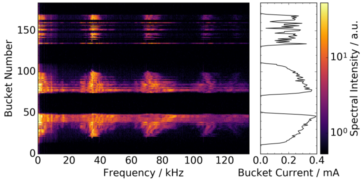

Theoretical description

Vlasov-Fokker-Planck equation describes the temporal development of the long. phase space:

$$\frac{\mathrm{d}\psi}{\mathrm{d}\theta} = \frac{\partial\psi}{\partial\theta} + \frac{\partial\mathcal{H}}{\partial p}\frac{\partial\psi}{\partial q} - \frac{\partial\mathcal{H}}{\partial q}\frac{\partial\psi}{\partial p} = \beta_\mathrm{d}\frac{\partial}{\partial p}\left(p\psi + \frac{\partial\psi}{\partial p}\right)$$

$$\mathcal{H}(q,p,\theta) = \underbrace{\mathcal{H}_l(q,p,\theta)}_{\text{unperturbed}} + \underbrace{\mathcal{H}_c(q,\theta)}_{\text{collective}}$$

$$= \frac{1}{2}\left(q^2+p^2\right) + \frac{ef_\mathrm{rev}}{\sigma_E f_{\mathrm{s},0}}\int_q^\infty V_c(q',t)\,\mathrm{d}q'$$

$$= \frac{1}{2}\left(q^2+p^2\right) + \frac{ef_\mathrm{rev}}{\sigma_E f_{\mathrm{s},0}}\int_q^\infty\int_{-\infty}^\infty \varrho(f)\,Z(f)\,e^{i2\pi fq'}\,\mathrm{d}f\,\mathrm{d}q'$$

Simulated phase space

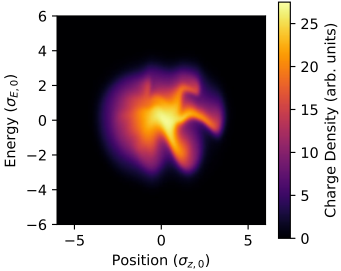

For the micro-bunching instability the impedance is dominated by the CSR impedance $Z_\mathrm{CSR}(f)$.
For most simulations either the parallel plates (shielded) or the free-space (no shielding) model are used.
e.g. [12, 19, 20, 21, 22]

Simulation with VFP solver

Inovesa

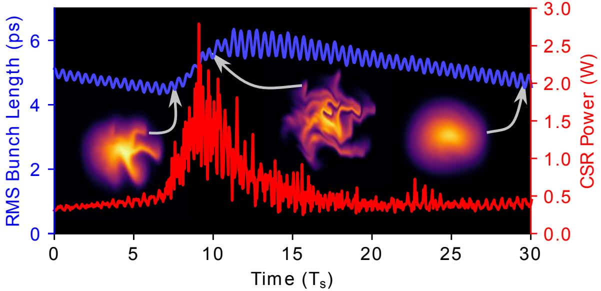

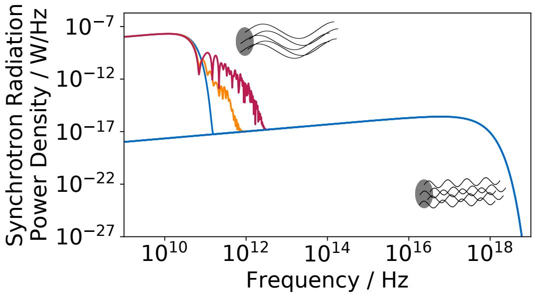

- Substructures in charge distribution
- Fluctuations of bunch profile due to synchrotron motion
- Dynamic growing and damping of substructures
- Bursts in emitted CSR power due to changes in emitted CSR spectra
- Dynamics depend on various machine parameters as well as bunch current

Inovesa
https://github.com/Inovesa
doi:10.5281/zenodo.4446191

Diagnostics at KARA

- Observation of longitudinal dynamics
  - Emitted coherent radiation (THz range)
  - Longitudinal bunch profile (< ps resolution)
  - Horizontal bunch size
- Relevant time scales
  - Size of sub-structures (sub-)ps
  - Bunch spacing / rev. time 2 ns / 368 ns
  - Repetition rate of bursts ~ ms
  - Current dependent changes ~ seconds/hours
- Diagnostic requirements:
  - High resolution (ps)
  - High repetition rate (500 MHz / 2.7 MHz)
  - Long term observation (secs - hrs)
  - Possibility for synchronised acquisition

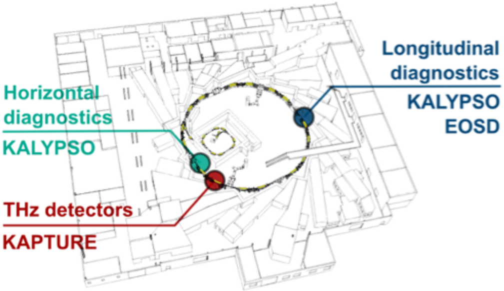

- KARA
  - Energy: 0.5 - 2.5 GeV
  - Circumference: 110.4 m
  - RF-frequency: 500 MHz
  - RMS bunch length: 45 ps, few ps (in short-bunch mode)

Fast THz detector and acquisition

Schottky barrier diode detectors

- Room temperature
- Covering 50 GHz - 1 THz
  $\longrightarrow$ Broad band quasi-optical or waveguide-coupled narrow band
- $>$ 4 GHz bandwidth $\longrightarrow$ Resolves light pulse of each bunch

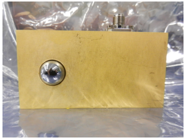

ACST GmbH

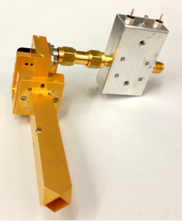

Virginia Diodes, Inc

KAPTURE - KArlsruhe Puls Taking and Ultrafast Readout Electronics

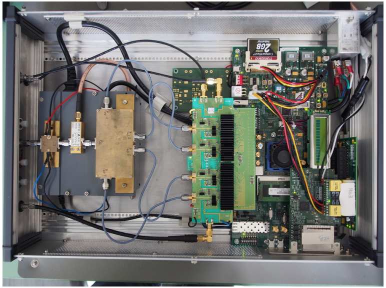

- Simultaneous monitoring of all 184 buckets
- Continuous turn-by-turn read-out of each bucket (500 MHz) $\longrightarrow$ 32 Gb/s
- Four sampling channels with 12-bit ADC each
- Adjustable delay for each channel in 3 ps steps
- Local sampling rate up to 300 GSa/s
- Alternative: read out multiple detectors simultaneously
- New: Version 2 with 8 channels and 1 GHz

M. Caselle, IPAC 2014 Dresden, THPME113

For more see talk by M. M. Patil FRXC03

Longitudinal bunch profile measurement

Electro-Optical Spectral Decoding

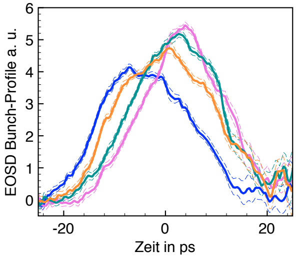

(N. Hiller, et al., IBIC 2014, MOPD17)

- Samples near field of electron bunch
- Initially developed for single-pass linacs
- Permanently installed in the KARA storage ring
- Operational in single-bunch operation
- Measures single-shot bunch profiles

KALYPSO KArlsruhe Linear arraY detector for MHz-rePetition rate SpectrOscopy

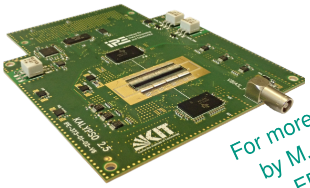

For more see talk by M. M. Patil FRXC03

(Courtesy by M. M. Patil)

- Line array (512, 1024 or 2048 pixel)
- Up to 10 Mfps @ 512 pixel
- Continuous data aquisition
- Combined with grating used as spectrometer

Energy spread studies

- Measure the horizontal bunch size σ_x in dispersive section of storage ring

$$\sigma_\delta = \frac{1}{D_x}\sqrt{\sigma_x^2 - \beta_x \cdot \epsilon_x}$$

- Incoherent synchrotron radiation (visible range)
- Radiation from 5° port at dipole magnet
- KALYPSO as fast line array detector
- turn-by-turn

KALYPSO

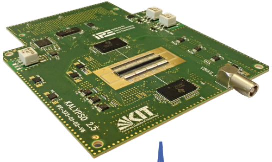

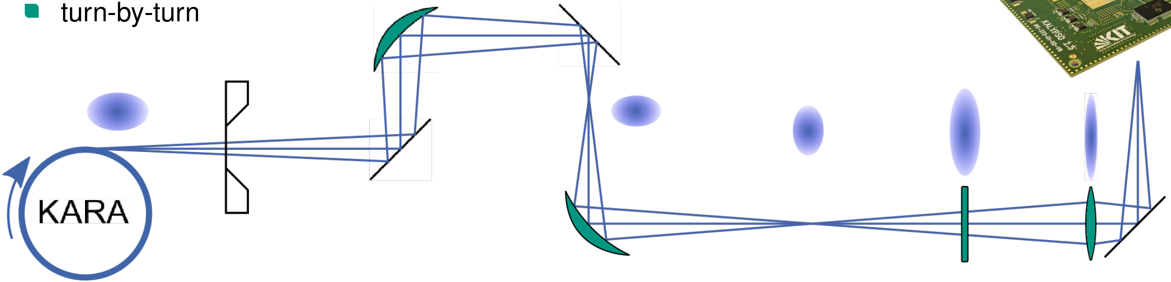

B. Kehrer, et al., IPAC19, doi:10.18429/JACoW-IPAC2019-WEPGW016

sketch, courtesy by Paul Schütze

Synchronous measurements

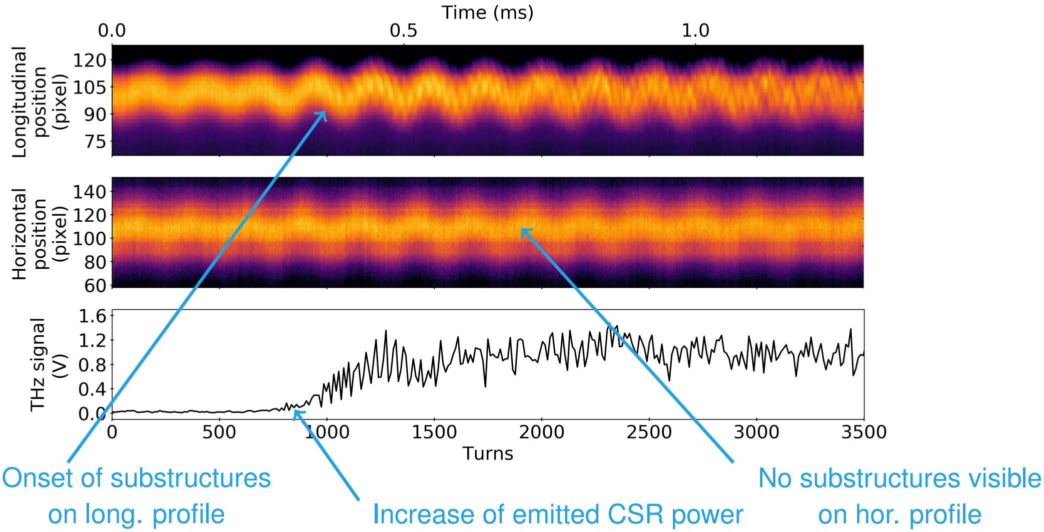

M. Brosi, et al., IPAC19, doi:10.18429/JACoW-IPAC2019-WEPTS015

Synchronous measurements

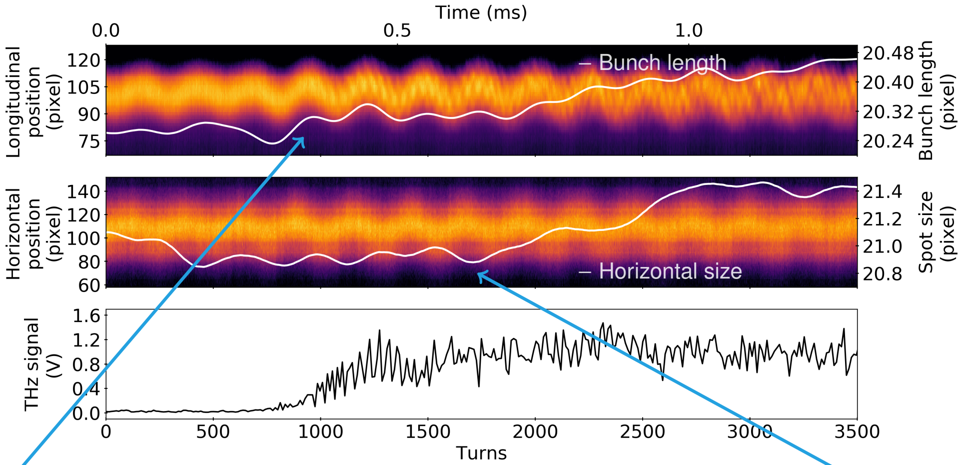

Bunch length and horizontal bunch size increase during burst

Onset of increase of bunch length

Delayed increase of hor. bunch size

M. Brosi, et al., IPAC19, doi:10.18429/JACoW-IPAC2019-WEPTS015

Synchronous measurements

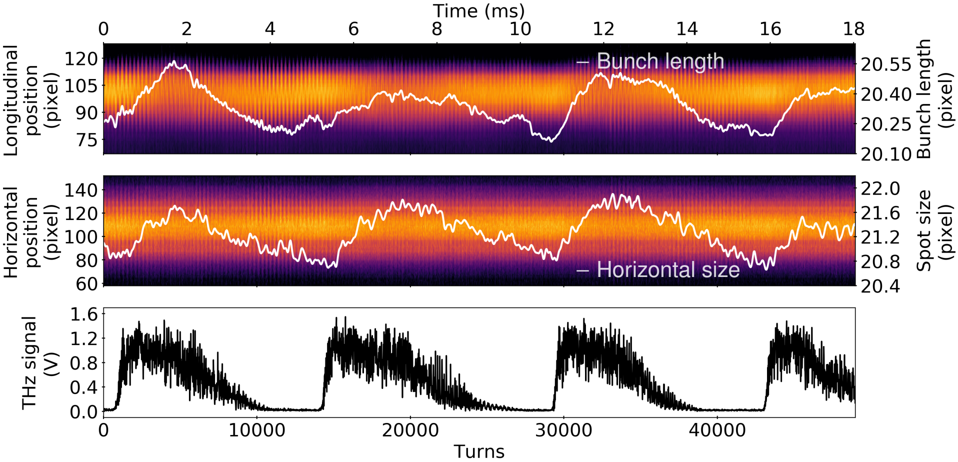

Bunch length and horizontal bunch size increase during burst

Slightly different shape but same repetition rate

M. Brosi, et al., IPAC19, doi:10.18429/JACoW-IPAC2019-WEPTS015

Synchronous measurements

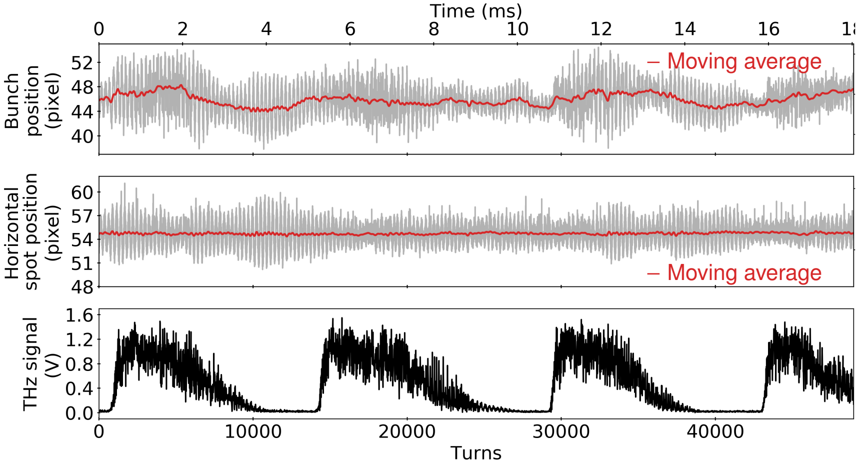

Small shift of long. position during burst

Ampiltude fits to expected shift due to additional loss by increased CSR emission

M. Brosi, et al., IPAC19, doi:10.18429/JACoW-IPAC2019-WEPTS015

Synchronous measurements

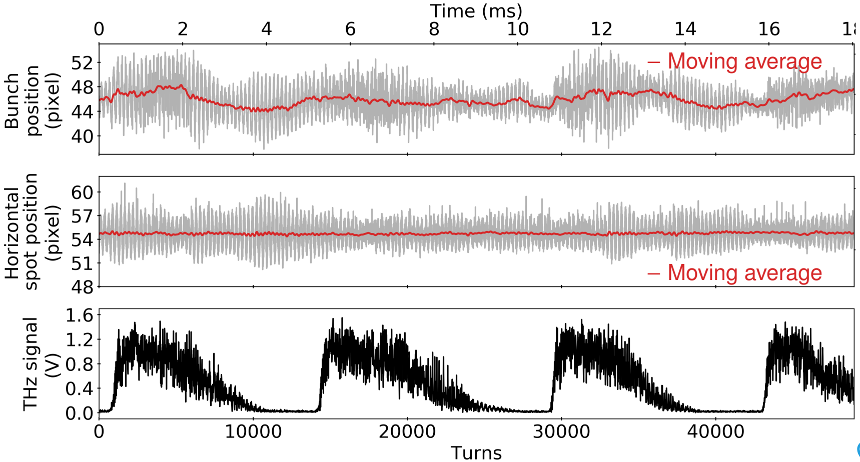

CSR as indicator for underlying dynamics

Small shift of long. position during burst

Ampiltude fits to expected shift due to additional loss by increased CSR emission

M. Brosi, et al., IPAC19, doi:10.18429/JACoW-IPAC2019-WEPTS015

THz measurements - bunch current dependence

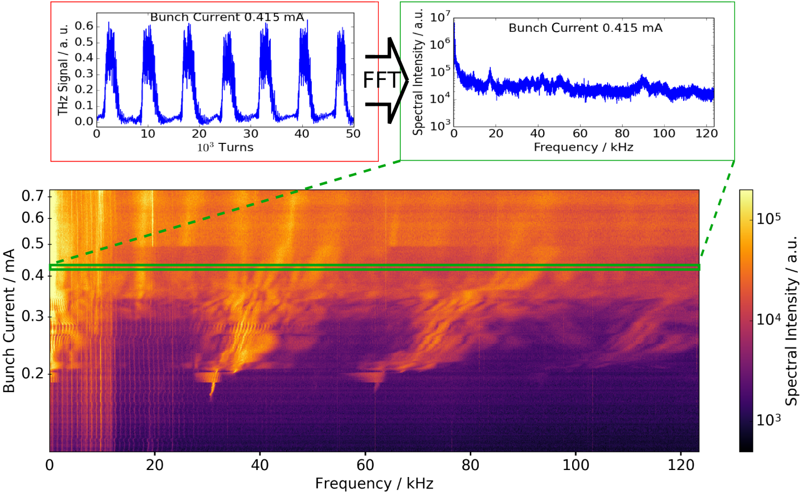

- Spectrogram: Representation of fluctuations in emitted CSR power as a function of bunch current

THz measurements - bunch current dependence

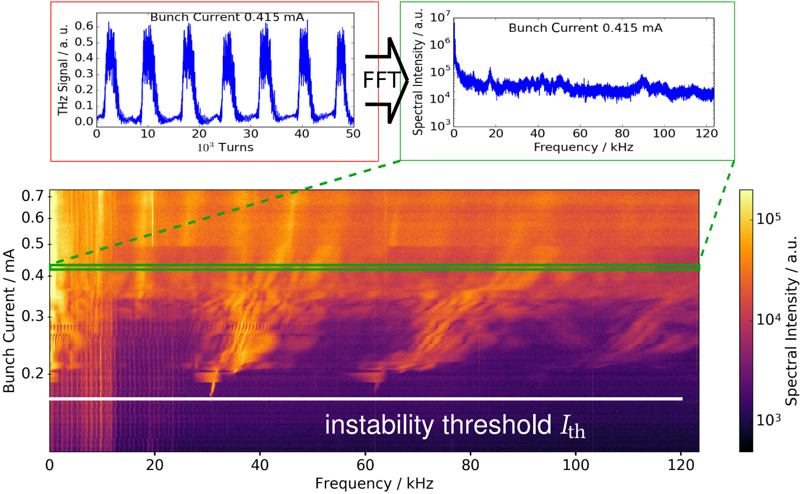

- Spectrogram: Representation of fluctuations in emitted CSR power as a function of bunch current
- Instability threshold visible as onset of fluctuations

THz measurements - bunch current dependence

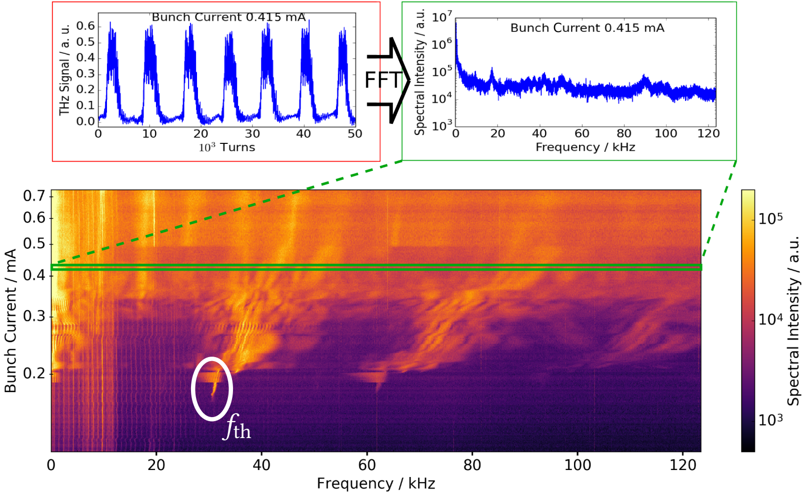

- Spectrogram: Representation of fluctuations in emitted CSR power as a function of bunch current
- Instability threshold visible as onset of fluctuations

THz measurements - bunch current dependence

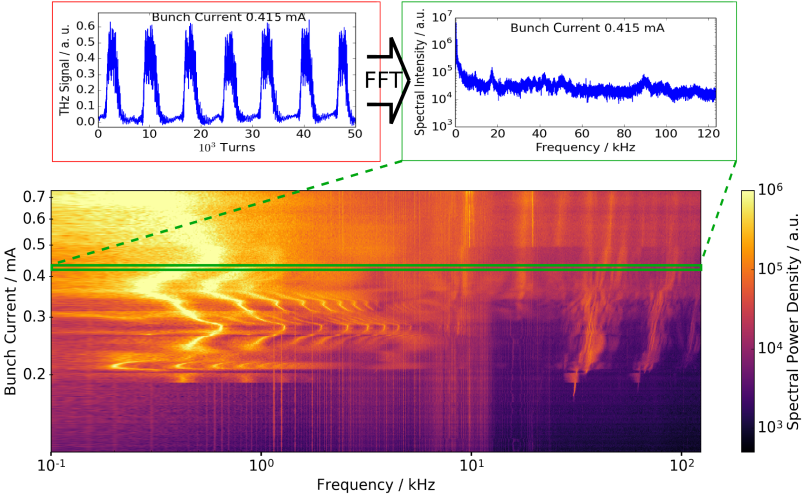

- Spectrogram: Representation of fluctuations in emitted CSR power as a function of bunch current
- Instability threshold visible as onset of fluctuations
- Low bursting frequency corresponds to repetition rate of outbursts

THz measurements - bunch current dependence

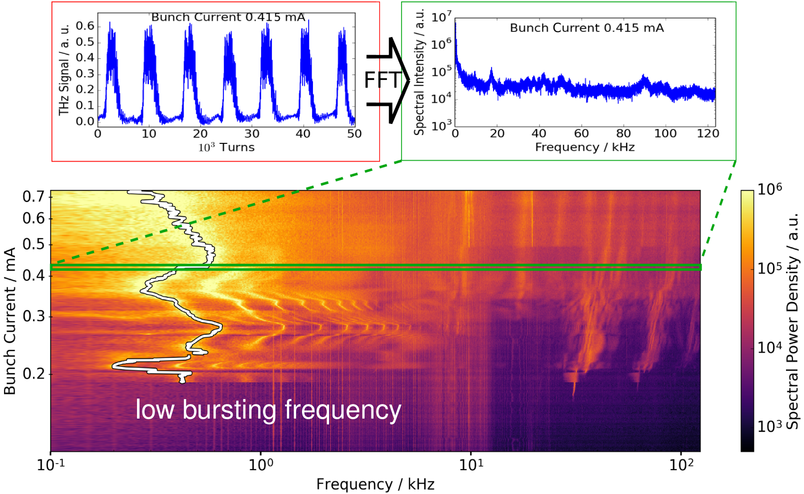

- Spectrogram: Representation of fluctuations in emitted CSR power as a function of bunch current
- Instability threshold visible as onset of fluctuations
- Low bursting frequency corresponds to repetition rate of outbursts

Influence of longitudinal damping time

on the low bursting frequency

- Reducing damping time with CLIC damping ring wiggler prototype at KARA
- No influence on threshold current observed
- Shift in low bursting frequency → due to faster damping of bunch length after outburst
- Dependency allows manipulation of dominant, low bursting frequency

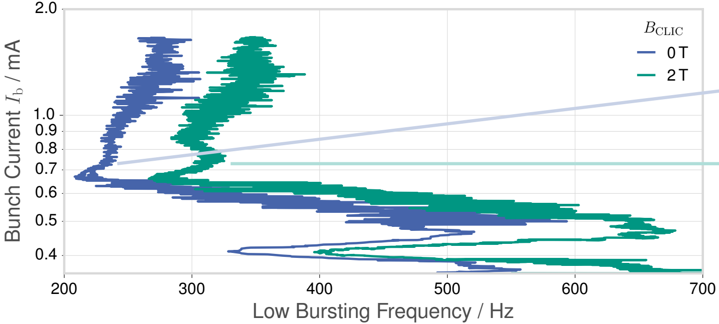

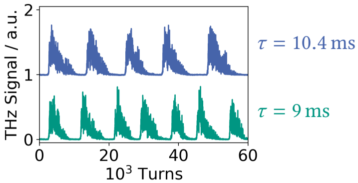

M. Brosi, et al., in Journal of Physics: Conference Series 1067.6 (2018).

Influence of operational parameters

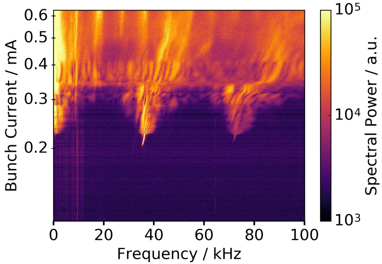

$\alpha_c \approx 5 \cdot 10^{-4}$, $V_{RF} = 4 \times 300\,\mathrm{kV}$
$\rightarrow f_s = 8.9\,\mathrm{kHz}$

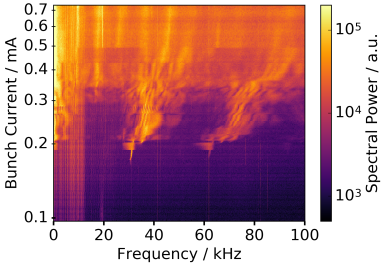

$\alpha_c \approx 5 \cdot 10^{-4}$, $V_{RF} = 4 \times 325\,\mathrm{kV}$
$\rightarrow f_s = 9.8\,\mathrm{kHz}$

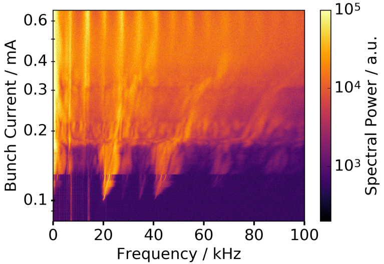

$\alpha_c \approx 3 \cdot 10^{-4}$, $V_{RF} = 4 \times 300\,\mathrm{kV}$
$\rightarrow f_s = 7.2\,\mathrm{kHz}$

- Fluctuation frequencies depend strongly on operational parameters
  - especially on momentum compaction factor (α_c) and acceleration voltage (V_{RF})
- Change in threshold current (I_{th}) and frequency at threshold (f_{th}) as well as in overall shape of spectrogram

M. Brosi, PhD thesis, KIT, 2020, doi:10.5445/IR/1000120018

Fluctuation frequency at threshold

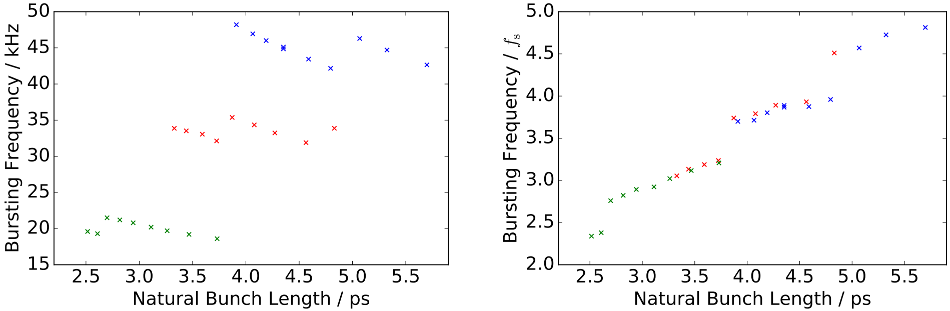

- Different operational parameters result in different frequencies
- Even when resulting in same natural bunch length
- When given in multiples of the synchrotron frequency it collapses to the same values
  $\Rightarrow f_{\mathrm{th}}/f_{\mathrm{s}}$ unambiguous for a given bunch length

M. Brosi, PhD thesis, KIT, 2020, doi:10.5445/IR/1000120018

Fluctuation frequency at threshold

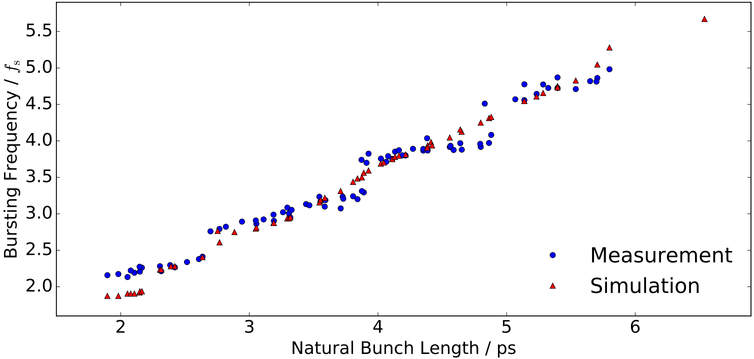

- Steps visible at approximately integer multiples
- Correlated to number of substructures in phase space
- Steps were also observed at CLS [4]
- Not clearly seen in VFP solver simulations based on pure parallel plates CSR model [23]

M. Brosi, PhD thesis, KIT, 2020, doi:10.5445/IR/1000120018

Instability threshold

- Main instability threshold [1]:

  $$(S_{\mathrm{CSR}})_{\mathrm{th}} = 0.5 + 0.12\ \Pi$$

  with shielding parameter $\Pi = \frac{\sigma_{\mathrm{z,0}}\,\rho^{1/2}}{h^{3/2}}$

  and CSR strength $S_{\mathrm{CSR}} = \frac{I_{\mathrm{n}}\,\rho^{1/3}}{\sigma_{\mathrm{z,0}}^{4/3}}$

  with normalized current $I_{\mathrm{n}} = \frac{\sigma_{\mathrm{z,0}} I_{\mathrm{b}}}{\alpha_{\mathrm{c}}\gamma\sigma_{\delta}^{2} I_{\mathrm{A}}}$,

  $\alpha_c = \frac{E f_{\mathrm{s}}^2 2\pi}{f_{\mathrm{RF}} f_{\mathrm{rev}} \sqrt{e^2 V_{\mathrm{RF}}^2 - U_0^2}}$ and $\sigma_{\mathrm{z,0}} = \frac{\alpha_{\mathrm{c}}\sigma_{\delta}}{2\pi f_{\mathrm{s}}}$
- Equation derived from fit to simulations
- Dip around $\Pi \approx 0.7$ due to weak instability
- Bounds predicted to depend not only on shielding, but also on $\beta = 1/(2\pi f_s \tau_d)$

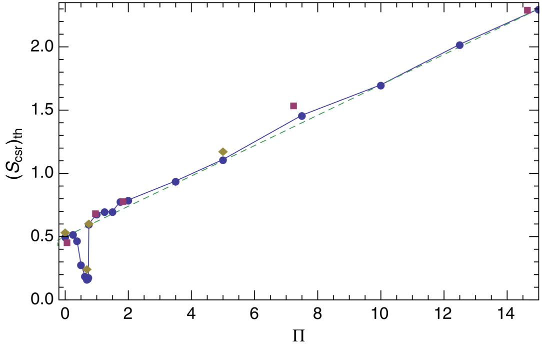

FIG. 3. For the CSR wake, threshold value of S_{csr} vs shielding parameter, $\Pi = \rho^{1/2}\sigma_{z0}/h^{3/2}$. Symbols give results of the VFP solver (blue circles), the LV code (red squares), and the VFP solver with twice stronger radiation damping (olive diamonds).

K. L. F. Bane and Y. Cai and G. Stupakov, Phys. Rev. STAB, 2010, Vol. 13, Nr. 10 [22]

Instability threshold

- Main instability threshold [1]:

$$(S_{\mathrm{CSR}})_{\mathrm{th}} = 0.5 + 0.12\,\Pi$$

with shielding parameter $\Pi = \frac{\sigma_{z,0}\,\rho^{1/2}}{h^{3/2}}$

and CSR strength $S_{\mathrm{CSR}} = \frac{I_{\mathrm{n}}\,\rho^{1/3}}{\sigma_{z,0}^{4/3}}$

with normalized current $I_{\mathrm{n}} = \frac{\sigma_{z,0} I_{\mathrm{b}}}{\alpha_{\mathrm{c}}\gamma\sigma_\delta^2 I_{\mathrm{A}}}$,

$$\alpha_c = \frac{E f_s^2 2\pi}{f_{\mathrm{RF}} f_{\mathrm{rev}} \sqrt{e^2 V_{\mathrm{RF}}^2 - U_0^2}} \quad \text{and} \quad \sigma_{z,0} = \frac{\alpha_c \sigma_\delta}{2\pi f_s}$$

- Equation derived from fit to simulations
- Dip around $\Pi \approx 0.7$ due to weak instability
- Bounds predicted to depend not only on shielding, but also on $\beta = 1/(2\pi f_s \tau_d)$

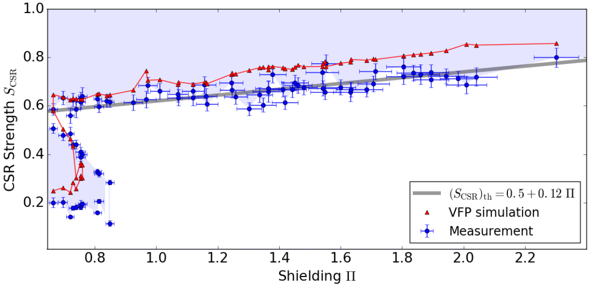

- Measurements fit linear scaling law
- Expected "Dip" due to weak instability observed
- Dedicated VFP simulations slightly, but systematically higher

M. Brosi et al., PRAB, 2019, doi:10.1103/PhysRevAccelBeams.22.020701

Threshold currents in multi-bunch operation

- Measured individual threshold currents during multi-bunch operation
- Standard deviation of measured thresholds: $\sigma\left(I_{\text{th}}\right) = 0.98\,\mu\text{A}$
- Uncertainty on bunch current measurement: $\sigma_{I_{\text{b,th}}} = 0.72\,\mu\text{A}$
- Remaining difference: $\sqrt{\sigma\left(I_{\text{th}}\right)^2 - \sigma^2_{I_{\text{b,th}}}} = 0.66\,\mu\text{A}$
- Further studies with even better current resolution necessary
- Small effect compared to changes in threshold current with operational parameters

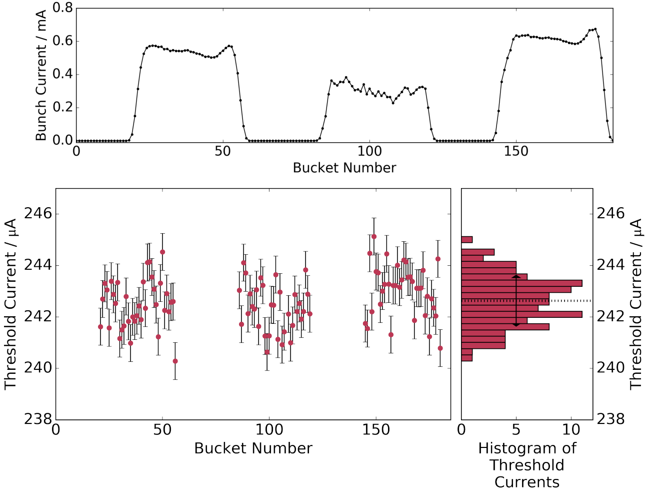

M. Brosi et al., IPAC'17, doi:10.18429/JACoW-IPAC2017-THOBA1.

“Snapshot" method with KAPTURE

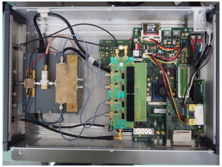

From THz signal to spectrogram with KAPTURE in seconds

- Cover beam current range with special filling pattern
- Read out time signal of each bunch with KAPTURE

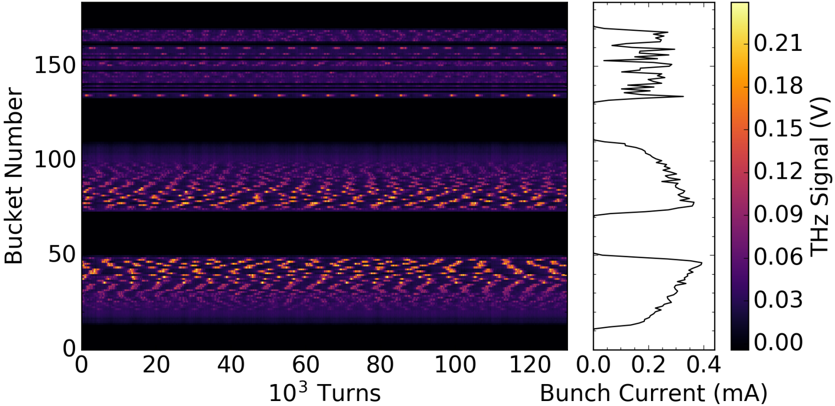

M. Brosi et al., Phys. Rev. Accel. Beams 19, 110701 (2016)

“Snapshot" method with KAPTURE

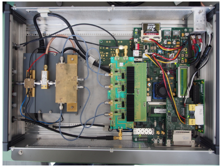

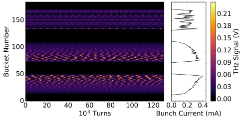

From THz signal to spectrogram with KAPTURE in seconds

- FFT for signal of each bunch

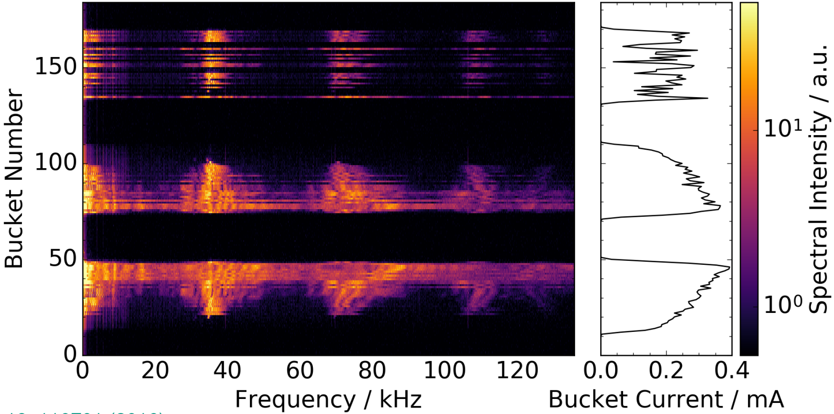

M. Brosi et al., Phys. Rev. Accel. Beams 19, 110701 (2016)

“Snapshot" method with KAPTURE

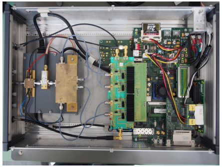

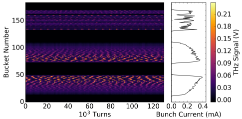

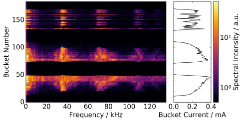

From THz signal to spectrogram with KAPTURE in seconds

- Sorted by bunch current

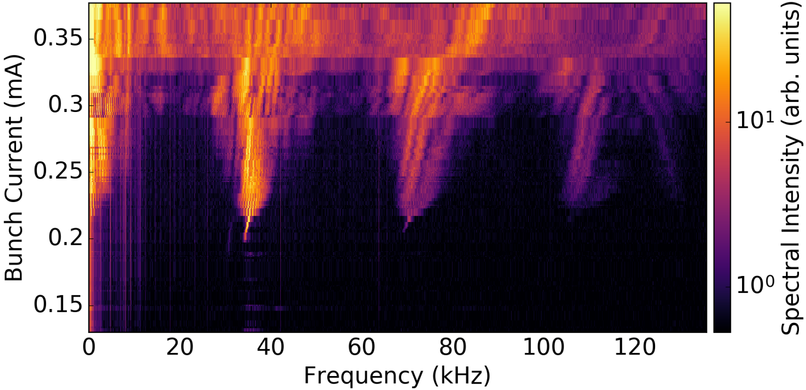

M. Brosi et al., Phys. Rev. Accel. Beams 19, 110701 (2016)

“Snapshot" method with KAPTURE

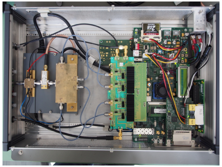

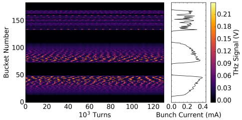

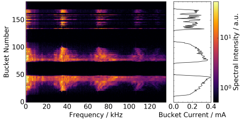

From THz signal to spectrogram with KAPTURE in seconds

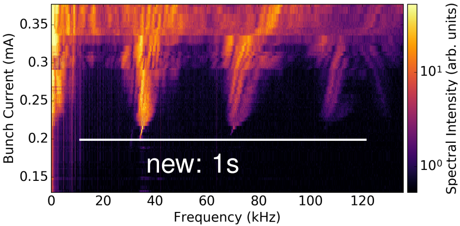

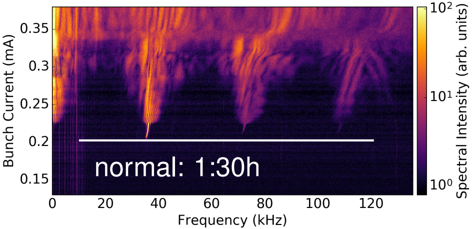

- Sufficient current resolution
- Drastically reduced measurement time
  $\longrightarrow$ Snapshot of machine status (concerning MBI)
- Fast scan of machine settings

M. Brosi et al., Phys. Rev. Accel. Beams 19, 110701 (2016)

Ongoing work on micro-bunching I

- Feedback via main RF-System or kicker cavity
  - PhLAM & SOLEIL, based on Pyragas time delayed feedback control (TDFC) [24]
  - KIT - KARA, based on reinforcement learning [25]
- Influence via additional impedances (impedance chamber) (collaboration between PhLAM, SOLEIL and KIT)
  S. Maier et al. these proceedings, TUPAB251
- Excitation of stronger micro-bunching using RF amplitude modulation T. Boltz et al. these proceedings, WEPAB233

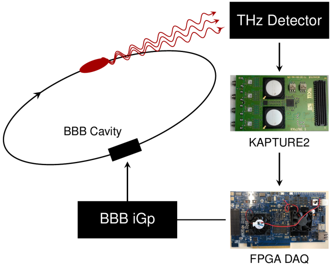

T.Boltz et al., ICALEPCS'19, doi:10.18429/JACoW-ICALEPCS2019-TUCPL06

Ongoing work on micro-bunching II

- Investigation of the micro-bunching instability at different operation modes e.g.:
  - Negative alpha operation [26] (with regards to low-emittance machines)
  - Injection during micro-bunching instability
- Steady State Micro-Bunching at MLS
  - Collaboration of Tsinghua University Bejing, HZB and PTB and later Shanghai Light Source
  - First proof of principle experiment performed [27]

    Talk by J. Feikes et al., MOXB01

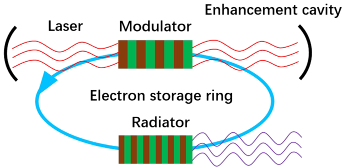

X. J. Deng et al., PRAB, Vol. 23, Iss. 4, doi:10.1103/PhysRevAccelBeams.23.044002

Summary

- Micro-bunching instability is longitudinal, collective instability caused by CSR self-interaction
- Leads to fluctuations in the bunch length, energy spread and emitted CSR power
- Observed and studied at many electron storage rings around the world
- Bunch-by-bunch and turn-by-turn diagnostics allows detailed study of the complex and nonlinear dynamics in the longitudinal phase space
- Fast snapshot measurement method provides "instant" characterization
- Ongoing studies:
  - Different operation modes
  - Influencing and control
  - Usability of CSR emission in form of Steady State Micro-Bunching

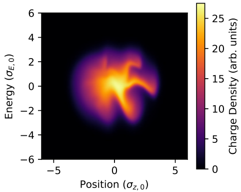

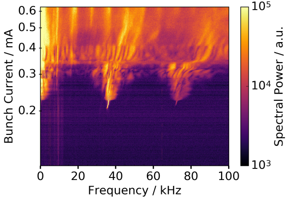

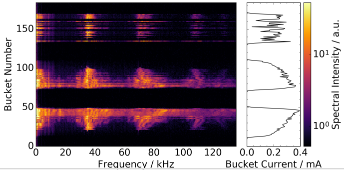

References I

[1] J. M. Byrd et al. “Observation of Broadband Self-Amplified Spontaneous Coherent Terahertz Synchrotron Radiation in a Storage Ring”. In: *Phys. Rev. Lett.* 89 (22 2002), p. 224801. DOI: 10.1103/PhysRevLett.89.224801.

[2] A.-S. Müller et al. “Far Infrared Coherent Synchrotron Edge Radiation at ANKA”. In: *Proceedings of the 2005 Particle Accelerator Conference*. 2005, pp. 2518–2520. DOI: 10.1109/PAC.2005.1591164.

[3] M Abo-Bakr et al. “Coherent emission of synchrotron radiation and longitudinal instabilities”. In: *Particle Accelerator Conference, 2003. PAC 2003. Proceedings of the*. Vol. 5. IEEE. 2003, pp. 3023–3025.

[4] B. E. Billinghurst et al. “Longitudinal bunch dynamics study with coherent synchrotron radiation”. In: *Phys. Rev. Accel. Beams* 19 (2 2016), p. 020704. DOI: 10.1103/PhysRevAccelBeams.19.020704.

[5] W Shields et al. “Microbunch Instability Observations from a THz Detector at Diamond Light Source”. In: *Journal of Physics: Conference Series* 357 (2012), p. 012037. DOI: 10.1088/1742-6596/357/1/012037.

[6] E. Karantzoulis et al. “Characterization of coherent THz radiation bursting regime at Elettra”. In: *Infrared Physics and Technology* 53.4 (2010), pp. 300–303. DOI: https://doi.org/10.1016/j.infrared.2010.04.006.

[7] A. Andersson et al. “Observation of coherent synchrotron radiation from a 1-mm electron bunch at the MAX-I storage ring”. In: *Accelerator-based Sources of Infrared and Spectroscopic Applications*. Ed. by G. L. Carr and P. Dumas. Vol. 3775. International Society for Optics and Photonics. SPIE, 1999, pp. 77 –87. DOI: 10.1117/12.366631.

[8] G. Wüstefeld et al. “Coherent THz Measurements at the Metrology Light Source”. In: *Proceedings of the 1st International Particle Accelerator Conference*. 2010, p. 2508.

[9] S. Hashimoto et al. “Observation of Coherent Synchrotron Radiation at Newsubaru”. In: *Proceedings of the 2005 Particle Accelerator Conference*. 2005, pp. 4188–4190. DOI: 10.1109/PAC.2005.1591760.

[10] G. Carr et al. “Investigation of coherent emission from the NSLS VUV ring”. In: *Particle Accelerator Conference, 1999. Proceedings of the 1999*. Vol. 1. IEEE. 1999, pp. 134–136.

[11] Y. Takashima et al. “Observation of Intense Bursts of Terahertz Synchrotron Radiation at UVSOR-II”. In: *Japanese Journal of Applied Physics* 44.No. 35 (2005), pp. L1131–L1133. DOI: 10.1143/jjap.44.l1131.

[12] B. V. Podobedov and R. H. Siemann. “Saw-tooth instability studies in the Stanford Linear Collider damping rings”. In: (1997), 4 p. URL: https://cds.cern.ch/record/336088.

[13] C. Evain et al. “Spatio-temporal dynamics of relativistic electron bunches during the micro-bunching instability in storage rings”. In: *EPL (Europhysics Letters)* 98.4 (2012), p. 40006. URL: http://stacks.iop.org/0295-5075/98/i=4/a=40006.

[14] U. Arp et al. “Spontaneous coherent microwave emission and the sawtooth instability in a compact storage ring”. In: *Phys. Rev. ST Accel. Beams* 4 (5 2001), p. 054401. DOI: 10.1103/PhysRevSTAB.4.054401.

[15] M. Ries et al. “THz Bursting Thresholds Measured at the Metrology Light Source”. In: *Proceedings of 2012 International Particle Accelerator Conference*. WEPPR046. 2012, p. 3030.

References II

[16] J. M. Byrd et al. “Broadband Self-amplified Spontaneous Coherent Synchrotron Radiation in a Storage Ring”. In: *Proc. 8th European Particle Accelerator Conf. (EPAC’02)* (Paris, France). JACoW Publishing.

[17] B. Podobedov and R. H. Siemann. “Signals from Microwave Unstable Beams in the SLC Damping Rings”. In: *Proc. 18th Particle Accelerator Conf. (PAC’99)* (New York, NY, USA). JACoW Publishing.

[18] E. Roussel et al. “Observing microscopic structures of a relativistic object using a time-stretch strategy”. In: *Scientific Reports* 5.1 (2015), p. 10330. DOI: `10.1038/srep10330`.

[19] R. L. Warnock and J. A. Ellison. “A General method for propagation of the phase space distribution, with application to the sawtooth instability”. In: *The physics of high brightness beams. Proceedings, 2nd ICFA Advanced Accelerator Workshop, Los Angeles, USA, November 9-12, 1999*. 2000, pp. 322–348. URL: `http://www-public.slac.stanford.edu/sciDoc/docMeta.aspx?slacPubNumber=SLAC-PUB-8404`.

[20] G. Stupakov and S. Heifets. “Beam instability and microbunching due to coherent synchrotron radiation”. In: *Phys. Rev. ST Accel. Beams* 5 (5 2002), p. 054402. DOI: `10.1103/PhysRevSTAB.5.054402`.

[21] M. Venturini and R. Warnock. “Bursts of Coherent Synchrotron Radiation in Electron Storage Rings: a Dynamical Model”. In: *Physical Review Letters* 89 (2002), p. 224802.

[22] K. L. F. Bane et al. “Threshold studies of the microwave instability in electron storage rings”. In: *Phys. Rev. ST Accel. Beams* 13 (10 2010), p. 104402. DOI: `10.1103/PhysRevSTAB.13.104402`.

[23] P. Kuske. “Short Bunches at the Transition From Strong to Weak Longitudinal Instability”. In: *Proc. of International Particle Accelerator Conference (IPAC’17), Copenhagen, Denmark, 14-19 May, 2017* (Copenhagen, Denmark). International Particle Accelerator Conference 8. Geneva, Switzerland: JACoW, 2017, pp. 3696–3699. DOI: `10.18429/JACoW-IPAC2017-THPAB007`.

[24] C. Evain et al. “Stable coherent terahertz synchrotron radiation from controlled relativistic electron bunches”. In: *Nature Physics* 15.7 (2019), pp. 635–639. DOI: `10.1038/s41567-019-0488-6`.

[25] T. Boltz et al. “Accelerating Machine Learning for Machine Physics (an AMALEA-project at KIT)”. In: *Proc. ICALEPCS’19* (New York, NY, USA). International Conference on Accelerator and Large Experimental Physics Control Systems 17. JACoW Publishing, Geneva, Switzerland, Aug. 2020, pp. 781–788. DOI: `10.18429/JACoW-ICALEPCS2019-TUCPL06`.

[26] P. Schreiber et al. “Status of Operation With Negative Momentum Compaction at KARA”. In: *Proc. 10th International Particle Accelerator Conference (IPAC’19), Melbourne, Australia, 19-24 May 2019* (Melbourne, Australia). International Particle Accelerator Conference 10. Geneva, Switzerland: JACoW Publishing, 2019, pp. 878–881. DOI: `10.18429/JACoW-IPAC2019-MOPTS017`.

[27] X. Deng et al. “Experimental demonstration of the mechanism of steady-state microbunching”. In: *Nature* 590.7847 (2021), pp. 576–579. DOI: `10.1038/s41586-021-03203-0`.